LED optical excitation for the long pulse and lock-in thermographic techniques

S.G. Pickering[1], K. Chatterjee[2], D.P. Almond[1], S. Tuli[2]

[1]UK Research Centre in NDE, Department of Mechanical Engineering, University of Bath, Bath BA2 7AY, UK.

[2]Centre for Applied Research in Electronics, Indian Institute of Technology, Delhi 110016, India

Email: S.G.Pickering@bath.ac.uk

Tel: +44 (0)1225 384801

Fax: +44 (0)1225 386928

Abstract

High power light emitting diode (LED) arrays have been investigated as excitation sources for long pulse and lock-in thermography. Images of artificial defects in a carbon fibre reinforced plastic (CFRP) composite sample are compared, by image contrast signal-to-noise ratio estimates, with those obtained using conventional incandescent flash and lock-in excitation sources. The LED arrays had to be mounted on heat sinks with active cooling in to prevent them exceeding their thermal tolerance. Despite this cooling the LED arrays were still found to emit some IR radiation, although far less than conventional incandescent light sources.

Keywords: infrared thermography, thermal imaging, thermal wave methods

1. Introduction

Pulsed transient thermography [e.g. 1, 2, 3] and lock-in thermography [e.g. 4, 5] are the most commonly used thermographic NDT&E techniques. The two techniques are distinctly different but are used for very similar component/structure inspection applications. Their defect detection capabilities are similar, i.e. the detection and imaging of broadly planar defects lying a short distance below the surface, e.g. delaminations in composites or adhesion defects in surface coatings. For pulsed transient thermography, the surface of the part to be inspected is flash heated by one or more high energy optical flash lamps or long pulse heated for a number of seconds using high power incandescent lamps, whilst for lock-in thermography the surface is heated periodically by modulated high power incandescent lamps for periods that may last for hundreds of seconds.

The technique of pulsed transient thermography involves using a high intensity pulse of light to heat the surface of a test piece via the photothermal effect. Both very short duration (~1ms) flashes and longer duration (seconds) pulses can be employed, depending on the sample thermal properties and defect depth.

Very short duration flashes are the preferred excitation method as sample thermal contrast caused by sub-surface defects is not obscured by the heat pulse. Depending on the sample thermal properties and defect depth, longer pulses (on the order of seconds) can also be employed. Long pulse testing has the advantage that the excitation sources are generally far simpler and cheaper than those required to generate fast flash excitation.

The test piece surface temperature is recorded by an infrared camera and computer system as it decays due to heat being conducted into the part after its deposition on the surface. Sub-surface defects reduce the conduction of heat away from the surface and therefore reduce the surface cooling rate compared to that occurring over non-defective regions. Consequently, a surface temperature contrast develops over a defect that can be used to detect a defective region. Alternatively, theoretical thermal decay predictions for defect free solids can be compared with the observed decay profiles to determine whether the sample contains sub-surface defects [6, 7].

In lock-in thermography, the sample is heated periodically, typically using a number of sinusoidally modulated tungsten-halogen flood lamps. Thermal images of the sample are recorded throughout the heating period, which lasts for at least one full excitation cycle. The magnitude of the periodic temperature change at the surface and its phase with respect to the applied modulated heating is then extracted by post-processing the recorded image data. After post-processing, the result of a test consists of just two images – a magnitude and a phase image.

With conventional flash or long-pulse heating using flash tubes or incandescent lamps, the tube/lamps and shroud continue to emit IR radiation even after they have been switched off. This additional IR radiation is directly reflected or scattered into the camera, causing surface reflectivity differences to dominate the early-time thermographic images, and also provides additional heating to the surface, which makes it difficult to measure and use the cool-down behaviour at these early times.

For lock-in thermographic testing the reflected IR radiation produces a large in phase component which is combined by superposition with the useful out-of-phase signal produced by the sample internal structure and thereby significantly reduces the observed phase signal making it both more difficult to detect and rendering theoretical predictions very inaccurate [8, 9, 10].

Recent developments in light emitting diode (LED) technology have led to high power density LED units, which are comparable with incandescent lamps in terms of brightness while being more compact, having lower power consumption and producing little or no infra-red radiation.

Low power, compact and highly controllable LED arrays are potentially ideal for thermographic NDE applications due to their portability and ability to be used to inspect components with constrained access. The fact that LED arrays produce little or no IR radiation is also of particular interest for thermographic NDE.

This paper investigates the use of high power LED arrays for pulse and lock-in thermography. Long pulse LED excitation is compared with conventional flash thermographic excitation and square wave lock-in LED excitation is compared with conventional incandescent lamp lock-in excitation. An objective comparison is made of the signal to noise ratios (SNR) produced by the different techniques.

2. Test Equipment

2.1. Test sample

Figure 1 shows a diagram of the CFRP test sample used for this testing containing flat-bottomed back-drilled hole defects at depths ranging from 0.25mm to 2.75mm in steps of 0.25mm. Only the 6mm and 4mm diameter defects were considered in this work.

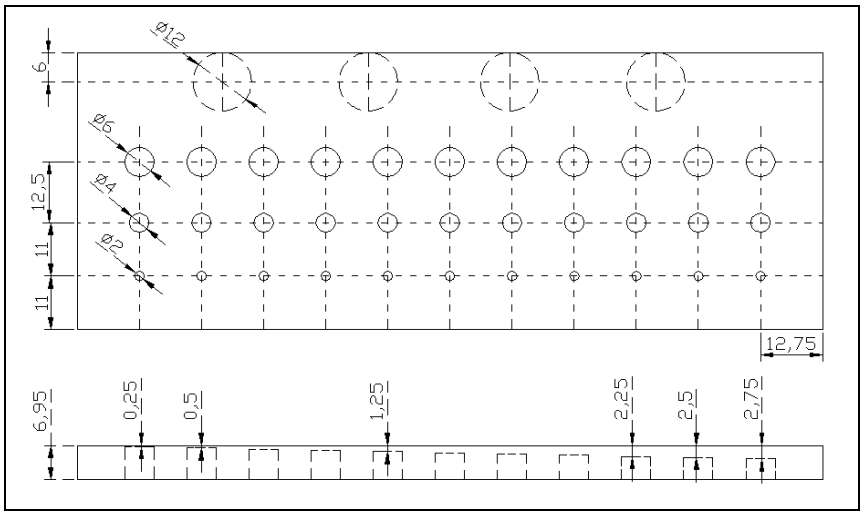

Figure 1 – CFRP composite test sample (all dimensions in mm)

2.2. IR Camera equipment

For all testing a TWI ThermoScope system using an Indigo Merlin camera was used. The ThermoScope system is an integrated pulsed thermographic system employing a medium wavelength infrared camera and an

integrated flash heating system which produces a pulse of light lasting ~3ms with an electrical energy of approximately 2kJ. The Indigo Merlin is an electrically cooled InSb Focal Plane Array (FPA) camera with 12-bit digital output and a resolution of 320x256 (width x height). The camera has a maximum framerate of 60Hz and an NEdT of less than 25mK (and typically <18mK) [11].

2.3. High Power Light Emitting Diode Arrays

The LED arrays used in this work are 16W units produced by Litewave Ltd. These are claimed to produce optical flux approximately equivalent to that produced by a 45 to 50W incandescent Halogen lightbulb [12]. These units can be driven from a 12V supply, which means their power supply can be made portable quite easily.

Figure 2 shows a picture of a single LED array unit. The overall LED array unit size is 17.5 mm x 28 mm with a thickness of 1.4mm. The LED emitter area in the centre measures 12 mm x 12 mm. The small size of these units is important both for potential use in confined areas and also in order to provide sufficiently high optical intensity and therefore photothermal heating of sample surfaces.

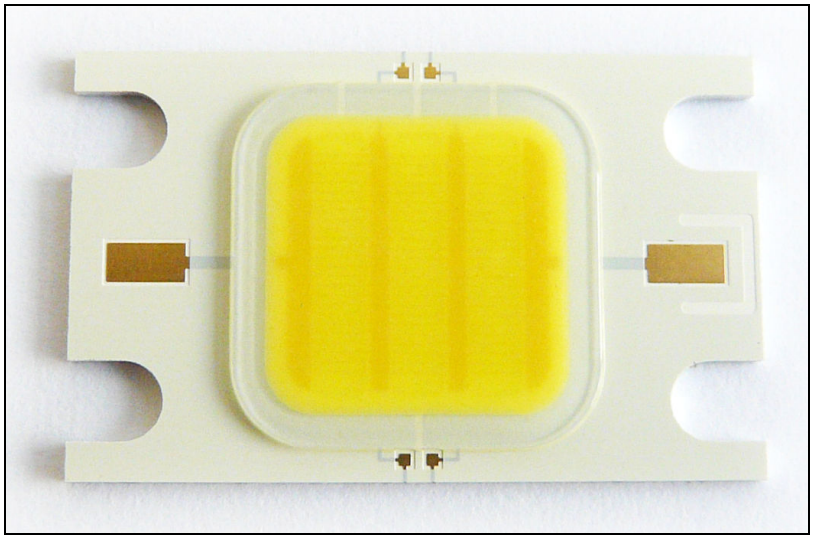

Figure 2 – Litewave LED array (image courtesy of Litewave Ltd.)

While LEDs are highly efficient and therefore produce little excess heat compared with incandescent light sources, it is recommended by the manufacturer that each LED array unit is mounted on a heat sink to ensure that when used they do not exceed their thermal tolerance limit of 120°C. In the case of the testing reported in this paper, it was important to keep the temperature considerably lower than the thermal tolerance limit, and to

disperse any excess heat away from the part being tested to ensure that no IR radiation would be generated by the LED array to interfere with the signal emitted by the test sample.

2.4. Lock-in Testing

For the lock-in testing four LED arrays were employed with each LED array screwed down on an individual computer Central Processing Unit (CPU) heatsink with cooling fins and an attached fan in order to maintain a low operating temperature. Due to the wide beam angle of the LED arrays (~140°), plano-convex lenses were mounted above each array element and held in place using synthetic rubber putty to produce a beam angle of approximately 30° which could then be focused on the sample. Figure 3 shows a picture of a single LED array attached to an aluminium heat-sink with a plano-convex lens attached to its front face.

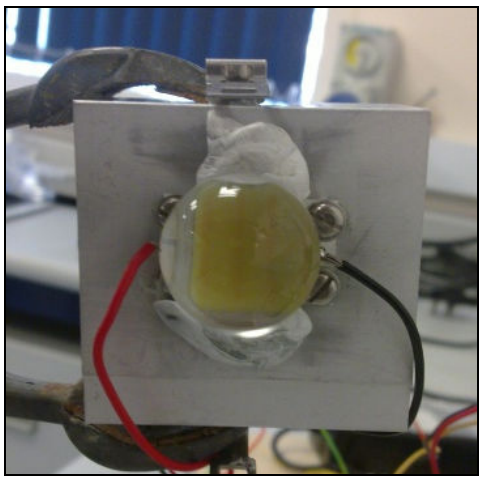

Figure 3 - LED array, lens and heatsink

(heatsink size 55x55mm, lens diameter 26mm)

A square-wave lock-in excitation signal was used instead of a sinusoid in order to simplify the control of the LED arrays at the expense of wasting some energy at harmonics of the lock-in frequency. For comparison, two 1kW tungsten-halogen flood lamps were driven using a signal generator and amplifier to produce a sinusoidal temperature flux on the sample surface. Water screens were used with the flood lamps to ensure that direct IR produced by the lamps was removed. This would otherwise have interfered with the phase response of subsurface defects significantly reducing the observed surface phase response [8, 9, 10].

Figure 4 shows the four LED arrays facing away from the camera with a gap in the centre where the IR camera would be placed. The cooling fans connected to the rear of the heat-sinks can be seen in this photograph, as can the large number of wires required to power the arrays and cooling fans.

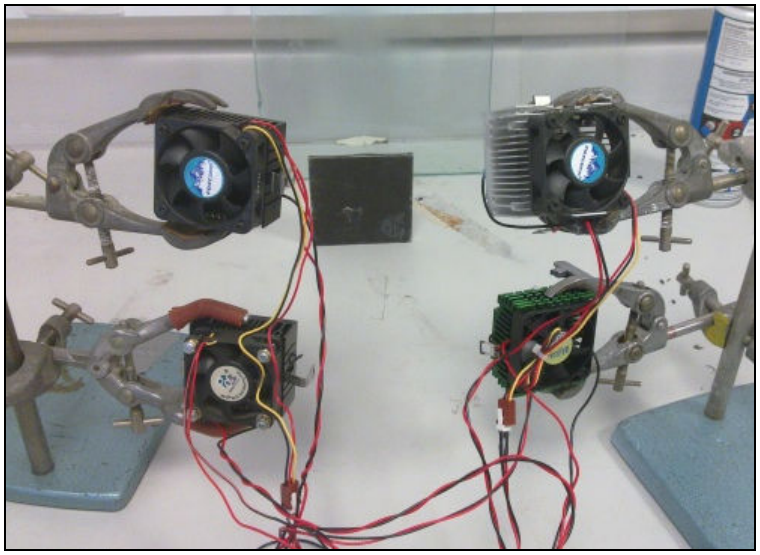

Figure 4 - LED arrays with cooling fans

Lock-in testing was performed at frequencies between 0.02 to 0.09Hz, with each test lasting for 1.5 periods in order to provide extra data that could be used to eliminate the sample background temperature rise over the course of the test [10].

2.5. Long pulse testing

The 4 LED array arrangement detailed above was tested for use in long-pulse excitation, however it was found that while this method produced good heating uniformity and allowed defects to be detected, in order to generate a useable surface heating only half the sample could be illuminated at once.

Due to the limited coverage area of the individually mounted LED arrays, it was decided to employ a total of 8 LED arrays. In order to make the setup sufficiently compact and easy to setup and use, each set of 4 LED arrays was mounted on a machined aluminium heatsink as shown in figure 6 below.

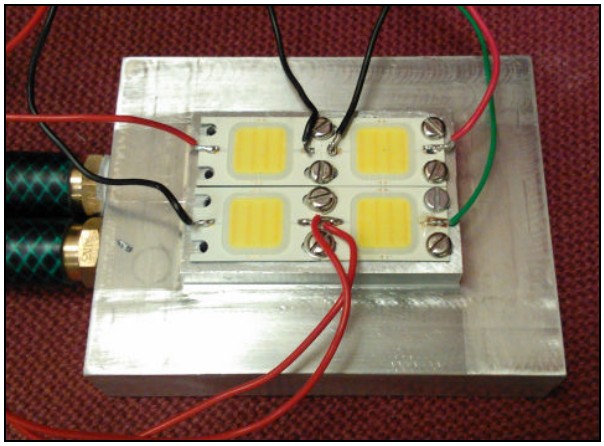

Figure 5 – 4x LED arrays mounted on water cooled heat sink

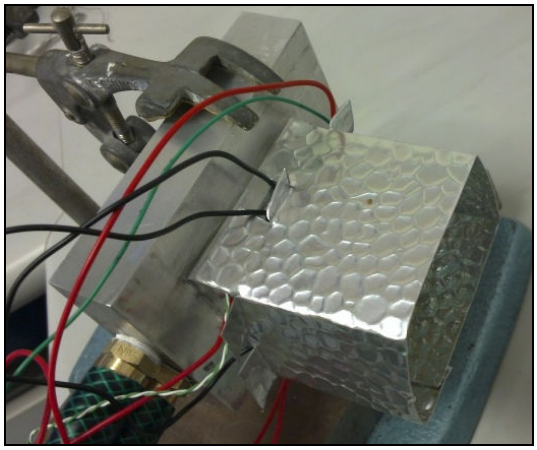

Figure 6 – Light-guide mounted on heat sink

As the arrays were now mounted close together it was not possible to fit the plano-convex lenses that were used for the lock-in testing, and therefore short (~50mm) aluminium light-guides were instead used to reduce the angular spread of the light to ensure that the majority was directed at the test samples (see figure 6). The use of 8 LED arrays with light-guides was found to produce a peak temperature rise of approximately 0.45°C for a 1s duration heating pulse over the entire sample surface compared which was approximately equal to that achieved over half the surface using 4 LED arrays with plano-convex lenses.

As the newly machined heat sinks lacked cooling fins and fans, water cooling was added to prevent overheating of the arrays if switched on for long periods. This system was not needed for individual long pulse tests as their duration is reasonably short, however if multiple consecutive tests were performed it was found useful to prevent a gradual temperatures rise of the heatsink and LED arrays.

For the testing the LED arrays were switched on for periods of between 1 and 15s to produce long pulse photothermal heating pulses.

3. Results

3.1. Lock-in thermographic testing

Figures 7 and 8, below, show typical phase images produced at a lock-in frequency of 0.06Hz using LED excitation and flood lamp excitation respectively. The grayscale values represent phase in degrees, with the non-defective parts of the sample set to a phase of -45° with respect to the excitation, as per the theoretical response of a semi-infinite solid. The row of 6mm diameter defects can be clearly seen as dark shapes across the middle of the samples, as can indications of the untested 12mm diameter defects at the top of the sample. The 4mm

defects can also be seen as feint dark regions below the row of 6mm defects. Of note is the fact that the first 4mm and 2mm defects (circles and labelled "A" on the left of the figures) are lighter than the background, indicating a phase lead with respect to the non-defective sample surface. This effect and the problems it causes as the phase of a defect crosses from a lead to a lag with respect to the non-defective sample is known as "blind frequencies" [8,9,10] and is caused by the transition from 1D to 3D heatflow due to the combination of defect size, depth and material properties.

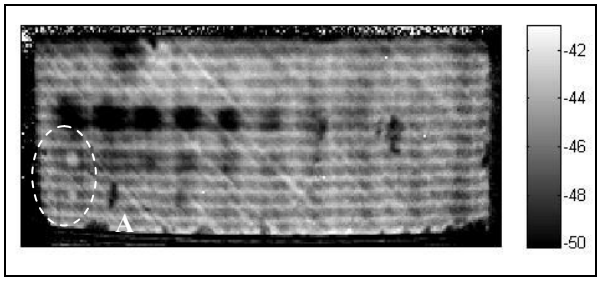

Figure 7 – Typical phase image (4x16W LED arrays with glass focusing lenses, f=0.06Hz)

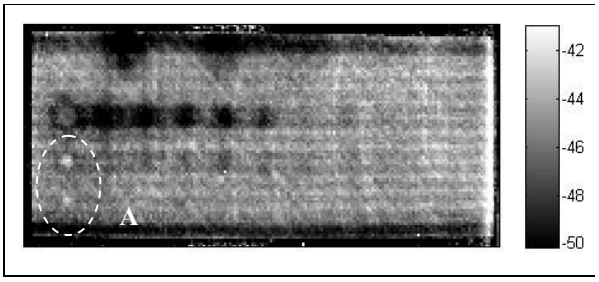

Figure 8 – Typical phase image (2x1kW flood lamps with water screens, f=0.06Hz)

Figure 9, below, shows the phase response SNR for lock-in testing on 6mm diameter defects using LED excitation; figure 10 shows comparable phase response SNR data using 2x1kW flood lamp excitation [as previously reported in 10].

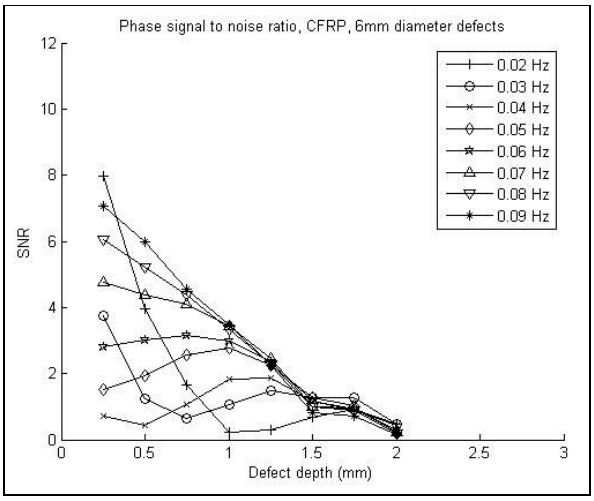

Figure 9 – LED array lock-in (6mm defects)

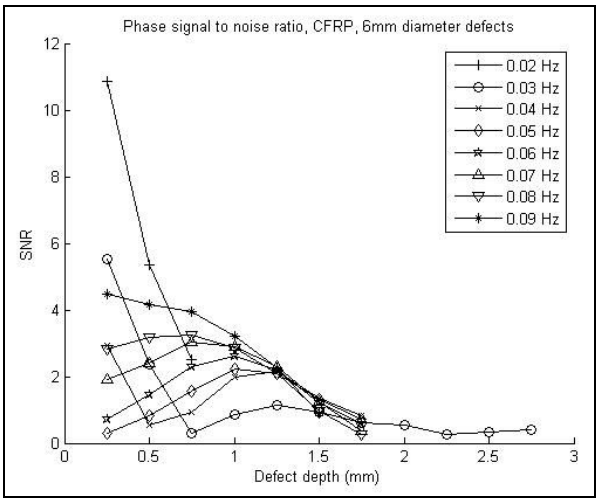

Figure 10 – 2kW flood lamp lock-in (6mm defects)

It can be seen that the results show largely the same trend over much of the defect depth range, with the mid-depth defects showing a dip where the "blind frequency" transition reduces the signal level as it moves from a phase lag to a phase lead with respect to the phase of the non-defective regions.

Of note is the fact that the deepest defects detected using LED excitation were at a depth of 2.0mm, while with flood lamp excitation defects of 2.75mm could be detected. This is thought to be due to the increased power of the flood lamps and their higher raw signal SNR allowing the responses of deeper defects to be detected. Nevertheless the difference is quite small considering the difference in electrical power of the two illumination systems (64W vs. 2kW).

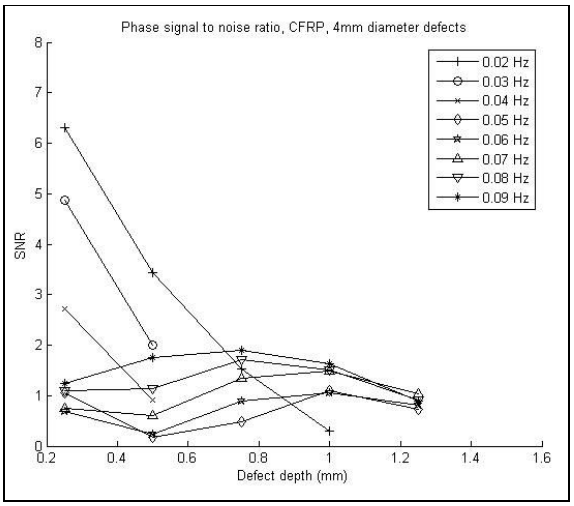

Figure 11 – LED array lock-in (4mm defects)

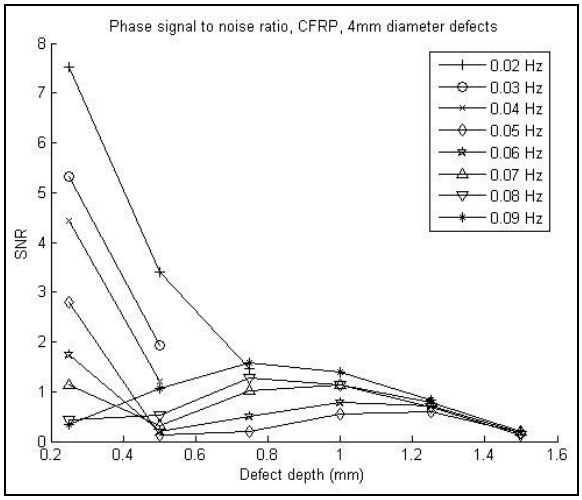

Figure 12 – 2kW flood lamp lock-in (4mm defects)

Figure 11 shows the phase response SNR for lock-in testing using LED excitation on 4mm diameter defects; Figure 12 shows comparable phase response SNR data using 2kW flood lamp excitation.

Again these results show similar trends and the effect of the "blind frequencies" is even more pronounced, producing two groupings of frequencies that produce similar trends: Lower frequencies produce a generally linear decrease in SNR with defect depth as would be expected if the heat transfer is behaving in a 1D manner, while the higher frequencies decrease then increase slightly as they pass through the "blind frequencies", in which little or no phase response is seen, due to the heat transfer in this case moving from 1D to 3D. Again one can see a relatively small difference in the maximum defect detection depth between the LED excitation and flood lamp excitation.

3.2. Long-pulse and flash thermographic testing

Figures 13 and 14, below, show typical contrast images produced by 15s LED excitation and flash excitation respectively. The images are not directly comparable due to the differences in heat time and elapsed time since heating, however they give an indication of the similarity of the images produced and in both cases multiple 6 and 4mm defects can be easily seen.

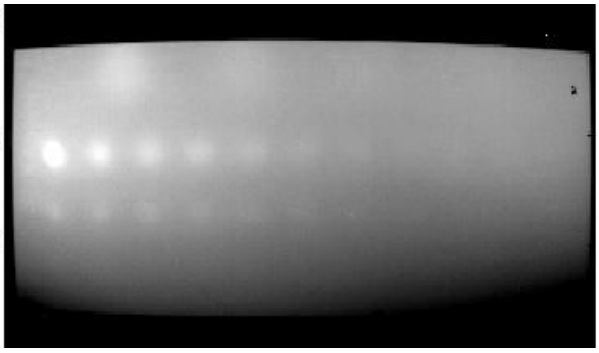

Figure 13 – Typical thermal contrast image for 15s LED array long pulse heating (~0.1s after end of heating)

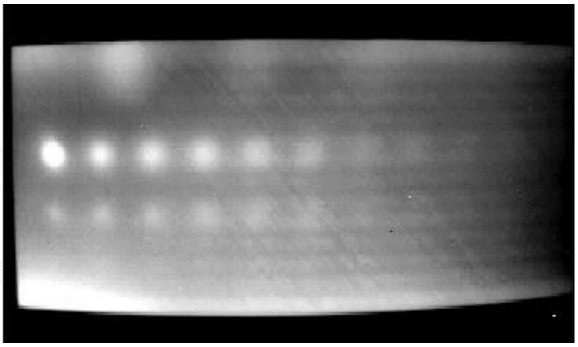

Figure 14 – Typical thermal contrast image for flash heating (~6s after flash)

Figure 15 shows the SNR of the 6mm diameter flat-bottomed back-drilled hole defects for LED array excitation times of between 1 and 15s and additionally the SNR for the defects when flash heated using the Thermoscope's integrated flash hood. Figure 16 similarly shows the SNR produced by the 4mm diameter defects for both LED long pulse and conventional flash heating.

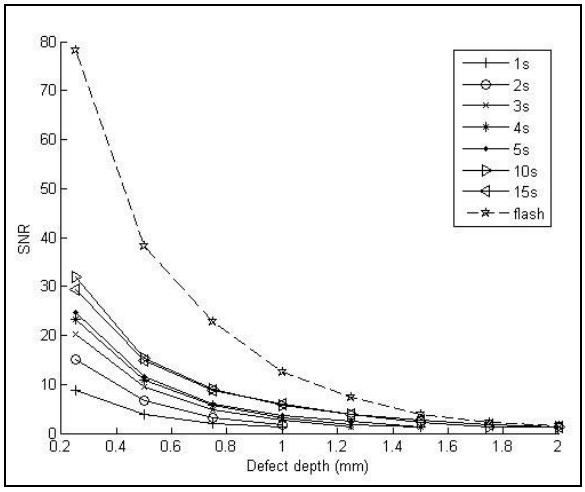

Figure 15 – Signal to noise ratio results for LED and flash heating of 6mm diameter defects in CFRP sample

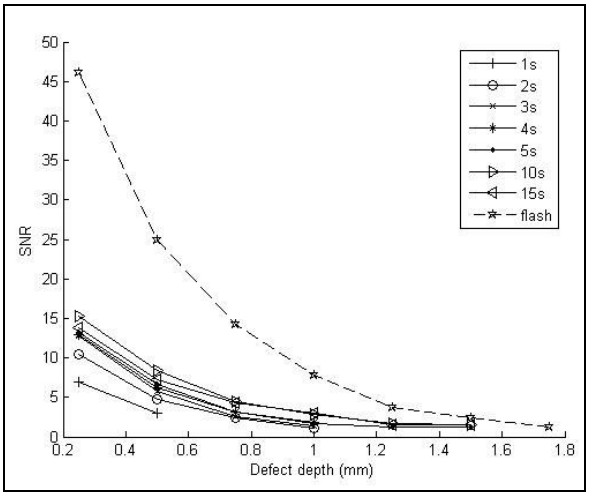

Figure 16 – Signal to noise ratio results for LED and flash heating of 4mm diameter defects in CFRP sample

In both cases one can see that, as might be expected, the long pulse excitation time is increased the SNR increases. It can be seen that the increase in SNR with longer excitation times is tending to converge and that while a heating time of 15s produces a slightly deeper maximum defect detection depths, it is otherwise largely comparable to the SNR results produced with 10s heating time.

It can be seen that flash excitation produces a significantly higher SNR for the shallowest defects, gradually converging to the same range as produced by the LED array long pulse heating for the deepest defects. A higher SNR is expected with flash excitation due to the higher energy deposited on the sample surface [13].

3.2.1. Presence of direct IR

While carrying out the LED long pulse testing it was noted that there was non-uniformity in the apparent surface temperature of the sample during the heating period. This can be seen in figure 17, below, in the form of brighter regions at the left and right ends of the sample.

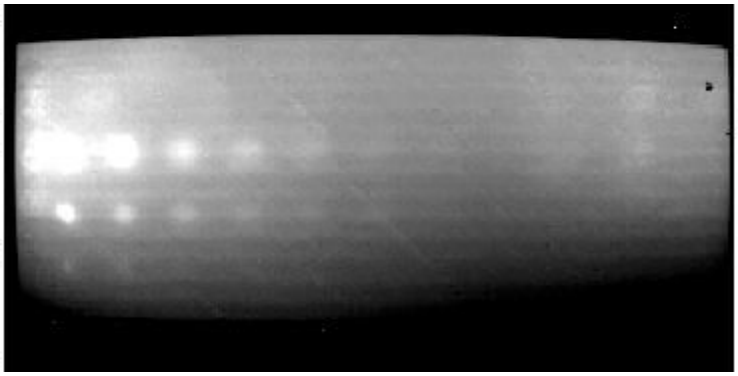

Figure 17 – Thermal image of CFRP sample during heating with LED arrays (heating time=10s)

One of the appeals of LED illumination for thermography is that they should produce "cold" light, without any IR component as would be produced by conventional incandescent lights. This would prevent two problems found in thermography: lock-in phase reduction caused by superposition of reflected and emitted IR energy [10]; and the "haze" effect caused by IR afterglow as seen in pulse thermography [14].

This non-uniformity is only present while the LED arrays are switched on, and therefore it can be concluded that it is the product of IR radiation being emitted from the hot LED arrays themselves. Despite being cooled, the arrays are not 100% efficient and therefore will become hot in operation; some of this energy is evidently emitted as IR along with the useful visible light.

While not a major problem, this does mean that additional care must be taken when analysing data recorded during the heating process in order to remove the effects of this non-uniform heating. This did not cause problems for the long pulse heating as the peak SNRs all occurred shortly after the heating had ended and this extra IR emission had therefore dissipated. It would have interfered with the results of the lock-in phase measurements; however for the lock-in testing any direct IR was serendipitously blocked by the glass plano-convex lenses which were being used to focus the light onto the sample.

4. Conclusions

It has been shown that long pulse and lock-in testing using high power LED array excitation produces comparable SNR results to those obtained using conventional incandescent flash and incandescent lamp lock-in methods.

While the very large SNR of shallow defects produced by the flash heating method produces little or no advantage over the LED arrays at these depths, as the depths increase the LED array SNRs soon approach some small multiple of the noise level. This is not a problem when using a cooled FPA camera, such as that employed in this testing, however this may be more problematic if used with a microbolometer camera which suffer from higher noise levels and therefore lower sensitivity than cooled FPA cameras [15].

It was found that despite their high efficiency and the assumption that they would emit "cold" (IR-free) light, high power LED arrays become hot when operating due to Joule heating. Heat sinks and active cooling are used to keep the LED arrays below their thermal tolerance limit, however the rate and/or location of the Joule heating sources is such that IR radiation is emitted in addition to the desired visible light. Without filtering direct IR emissions have been shown to generate interference in lock-in phase signals [10], and this problem was coincidentally avoided during in this work due to the use of thick glass focusing lenses, which absorbed the IR radiation preventing it from reaching the sample.

If a different arrangement were used for lock-in testing, such as the light-guides employed in the long pulse testing, it would be necessary to use glass/water screens to prevent interference from the direct IR emissions, as were used for the incandescent flood lamp comparison testing.

Unfortunately the requirement to mount the LED arrays on heatsinks with either sufficient heat capacity and/or active cooling, and the need to block direct IR while performing lock-in testing negate the most interesting of the advantages that it had been thought LED arrays would provide over incandescent light sources, namely compactness, portability and the ability to produce light without any IR component.

5. Acknowledgements

This work formed part of the Core Research Programme of the UK Research Centre in NDE (RCNDE) supported by the Engineering and Physical Science Research Council (EPSRC), UK, and was carried out in collaboration with the Indian Institute of Technology (IIT) Delhi as part of a UK-India Education and Research Initiative (UKIERI) project.

6. References

1. Milne JM, Reynolds WN. *The non-destructive evaluation of composites and other materials by thermal pulse video thermography*. Proc. Soc. Photo-Opt. Instrum. Eng, 1985. pp.119-122.

2. Lau SK, Almond DP, Milne JM. *A quantitative analysis of pulsed video thermography*. Non Dest. Testing Eval. Int. 24, 1991, pp.195-202.

3. Shepard S. *Advances in Pulsed Thermography*. A.E. Rozlosnik, R.B. Dinwiddie eds, Thermosense XIV, SPIE Proc. 4360, 2001: pp.511-515.

4. Busse G, Wu D, Karpen W. *Thermal wave imaging with phase sensitive modulated thermography*. Journal of Applied Physics, April 15, 1992, Volume 71, Issue 8, pp.3962-3965.

5. Busse G. *Optoacoustic phase angle measurement for probing a metal*. Appl. Phys. Lett. 35, 1979, pp.759-60.

6. Pickering SG, Almond DP. *Automated defect detection for pulsed transient thermography*. in Review of Progress in QNDE 2006, Vol. 26B, eds. D.O. Thompson and D.E. Chimenti (AIP Conference Proceedings, New York, 2006) , pp.1585-1592.

7. Shepard SM, Hou Y, Ahmed T, Lhota JR. *Reference-free interpretation of flash thermography data.* Insight - Non-Destructive Testing and Condition Monitoring, Vol. 8, Issue 5, May 2006, pp.298-301.

8. Bai W, Wong BS. *Evaluation of defects in composite plates under convective environments using lock-in thermography*. Meas. Sci. Technol., 2001, Vol. 12. pp. 142-150.

9. Wallbrink C, Wade SA, Jones R. *The effect of size on the quantitative estimation of defect depth in steel structures using lock-in thermography*. Journal of Applied Physics, 2007, Volume 101, Issue 10, pp. 104907-104907-8.

10. Pickering SG, Almond DP. (2008). Matched excitation energy comparison of the pulse and lock-in thermography NDE techniques, NDT & E International, Volume 41, Issue 7, October 2008, Pages 501-509. DOI:10.1016/j.ndteint.2008.05.007

11. Thermal Wave Imaging Inc. http://www.thermalwave.com/thermoscope.html

12. Litewave Ltd. http://www.litewave.co.uk/16w_led.asp

13. Almond, D. P., Pickering, S. G. *An analytical study of the pulsed thermography defect detection limit.* Journal of Applied Physics, 2012, 111 (9), 093510. DOI: 10.1063/1.4704684

14. Shepard SM, Young T. *Method and Apparatus for Thermographic Imaging using Flash Pulse Truncation*. 2007, US patent: US 7,186,981 B2.

15. Pickering SG, Almond DP. *An evaluation of the performance of an uncooled microbolometer array infrared camera for transient thermography NDE*. Nondestructive Testing and Evaluation, 2007, Volume 22, Issue 2 & 3 June 2007 , pp.63–70.